Mon. Not. R. Astron. Soc. **358,** 1240–1246 (2005) doi:10.1111/j.1365-2966.2005.08733.x

Confirmation of the effectiveness of submm source redshift estimation based on rest-frame radio–FIR photometry

Itziar Aretxaga,[1]★ David H. Hughes[1] and James S. Dunlop[2]

[1]*Instituto Nacional de Astrofísica, Óptica y Electrónica (INAOE), Aptdo. Postal 51 y 216, 72000 Puebla, Mexico*
[2]*Institute for Astronomy, University of Edinburgh, Royal Observatory, Edinburgh EH9 3HJ*

Accepted 2004 December 9. Received 2004 October 27; in original form 2004 August 20

ABSTRACT

We present a comparison between the published optical, infrared (IR) and CO spectroscopic redshifts of 15 (sub)mm galaxies and their photometric redshifts as derived from long-wavelength (radio–mm–far-IR) photometric data. The redshift accuracy measured for 12 submillimetre (submm) galaxies with at least one robustly determined colour in the radio–mm–far-IR regime is $\delta z \approx 0.30$ (rms). Despite the wide range of spectral energy distributions in the local galaxies that are used in an unbiased manner as templates, this analysis demonstrates that photometric redshifts can be efficiently derived for submm galaxies with a precision of $\delta z < 0.5$ using only the rest-frame far-IR to radio wavelength data.

Key words: surveys – galaxies: evolution – cosmology: miscellaneous – infrared: galaxies – submillimetre.

1 INTRODUCTION

The next generation of wide-area extragalactic submillimetre (hereafter submm) and mm surveys, for example from the *Balloon-borne Large Aperture Submillimetre Telescope* (*BLAST*, Devlin 2001), LABOCA on the Atacama Pathfinder Experiment (APEX[1]), the SCUBA 2 camera[2] on the James Clerk Maxwell Telescope (JCMT) and BOLOCAM-II on the Large Millimetre Telescope (LMT[3]), will produce large samples ($\sim 10^3$–10^5) of distant, luminous starburst galaxies. The dramatic increase in the number of submm-detected galaxies requiring follow-up observations makes it unreasonable to expect that a large fraction of their obscured or faint optical and infrared (IR) counterparts will have unambiguous, spectroscopically determined redshifts. An alternative method to efficiently and robustly measure the redshift distribution for large samples of submm galaxies is clearly necessary.

Given the underlying assumption that we are witnessing high rates of star formation in these submm galaxies, then we expect them to have the characteristic far-IR (FIR) peak and steep submm (Rayleigh–Jeans) spectrum which is dominated by thermal emission from dust heated to temperatures in the range ∼20–70 K by obscured young, massive stars. The observed radio–FIR luminosity correlation in local starburst galaxies (e.g. Helou, Soifer & Rowan-Robinson 1985), that links the radio synchrotron emission from supernova remnants with the later stages of massive star formation, is also expected to apply to the submm galaxies.

Thus, in recent years, a considerable amount of effort has been invested in assessing the accuracy with which these broad continuum features in the spectral energy distributions (SEDs) of submm galaxies at rest-frame mid-IR to radio wavelengths can be used to provide photometric redshifts (Hughes et al. 1998; Carilli & Yun 1999, 2000; Dunne, Clements & Eales 2000; Rengarajan & Takeuchi 2001; Yun & Carilli 2002; Wiklind 2003; Blain, Barnard & Chapman 2003). In a contribution to this general investigation, Hughes et al. (2002, hereafter Paper I) described Monte Carlo simulations that used a library of multifrequency template SEDs, derived from observations of local starbursts and AGN with a wide-range of FIR luminosities ($9.0 < \log L_{\rm FIR}/{\rm L}_{\odot} < 12.3$) and temperatures ($25 < T/{\rm K} < 65$), to measure the accuracy of photometric redshifts that could be derived from future 250-, 350- and 500-μm extragalactic surveys with BLAST and Herschel, and complementary 850-μm surveys from SCUBA. Aretxaga et al. (2003, hereafter Paper II) then applied the techniques described in Paper I to the catalogues of submm galaxies identified in various SCUBA surveys, and derived photometric redshifts for individual sources using existing radio–submm data.

In this paper we use new optical and IR spectroscopic observations of submm galaxies published by Chapman et al. (2003a), and Simpson et al. (2004) to update our previous comparison of spectroscopic and long-wavelength photometric redshifts (Paper II). In Section 2 we explain the selection criteria for the submm sources with spectroscopic redshifts included in our analysis, and demonstrate how the accuracy of the photometric redshift prediction varies according to the quality of the radio–mm–FIR photometric data. In Section 3 we discuss the significant agreement between the

★E-mail: itziar@inaoep.mx
[1] www.mpifr-bonn.mpg.de/div/mm/apex/
[2] www.roe.ac.uk/ukatc/projects/scubatwo/index.html
[3] www.lmtgtm.org

spectroscopic and photometric redshifts, and use these results to challenge the suggestion by Blain et al. (2003) that it is not possible to derive photometric redshifts with an accuracy of $dz \simeq \pm 0.5$ or better without adopting an unreasonably tight dispersion in the luminosity–temperature (L–T) relation or a limited range of SEDs in the analysis. Finally, our conclusions are summarized in Section 4.

The cosmological parameters adopted throughout this paper are $H_0 = 67\,\mathrm{km\,s^{-1}\,Mpc^{-1}}$, $\Omega_\mathrm{M} = 0.3$, $\Omega_\Lambda = 0.7$.

2 ANALYSIS

2.1 New spectroscopic redshifts for submm sources

Over the last year several new optical and IR spectroscopic redshifts have been published for submm sources (Chapman et al. 2003a; Simpson et al. 2004), enhancing substantially the number of sources available for checking the reliability of photometric estimates. Many of the submm galaxies selected for spectroscopic study have been extracted from the 8-mJy SCUBA survey (Scott et al. 2002), aided by deep follow-up observations with the Vert Large Array (VLA) (Ivison et al. 2002).

Of the 10 optical redshifts published by Chapman et al. (2003a), we include in our analysis only those five sources with photometric data of sufficient quality. We briefly discuss the SED properties of the excluded sources as follows.

(i) SMM105224.6+572119 ($z_\mathrm{opt} = 2.429$), also known as LE850.15 from the UK 8-mJy SCUBA survey of the Lockman Hole East, is rejected because the submm source has since been shown to be a spurious 850-μm detection. In Scott et al. (2002) this source was originally listed as a low signal-to-noise ratio (3.4σ) submm source, having been extracted from one of the more noisy regions of the 8-mJy maps. Subsequently it was highlighted by Ivison et al. (2002) to be very likely erroneous on account of its lack of a radio counterpart (despite its very bright apparent submm flux). The spurious nature of this source has been supported by the failure to detect the source in a reanalysis of the 8-mJy maps conducted as part of SHADES (Mortier et al. 2005; www.roe.ac.uk/∼ifa/shades), and by its non-detection in the IRAM MAMBO mm-wavelength maps of the 8-mJy Lockman East field (Greve et al. 2004).

(ii) SMM105207.7+571907 ($z_\mathrm{opt} = 2.698$) or LE850.12, also from the UK 8-mJy SCUBA survey, has a bright and statistically secure radio counterpart (Ivison et al. 2002). This object, however, is a known AGN, with strong, flat-spectrum, variable radio emission. Therefore, it must be excluded from the analysis presented here, which relies on the fitting of non-variable starburst-dominated spectral templates. As we show later no SED in our local template library can reproduce the high radio fluxes of this variable radio source at the spectroscopic redshift, and indeed, in Paper II we already reported that the SED could not be matched at any redshift with the local templates.

(iii) SMM123600.2+621047 ($z_\mathrm{opt} = 1.998$), whose position (J2000) corresponds to a 1.4-GHz radio source (123600.150+621047.17) in Richards (2000), has a spectrum which presumably arises from an optically faint ($I = 23.6$) VLA radio source that was followed up with submm photometry, but the robustness of the radio–submm association cannot be determined from the published information.

(iv) SMM131201.2+424208 ($z_\mathrm{opt} = 3.419$) and SMM131212.7+424423 ($z_\mathrm{opt} = 2.811$) still do not have published 1.4-GHz data from the SSA13 field (Fomalont et al., in preparation), and we therefore cannot reconstruct the radio–submm SED of this source.

In the analysis described in Section 2.2 we include the remaining five submm sources from the 8-mJy survey studied by Chapman et al. (2003a), namely N2850.1, N2850.4, N2850.8, LE850.6 and LE850.18, which have unambiguous radio identifications from Ivison et al. (2002). The spectroscopic redshifts for all these sources also appear to be secure, and indeed redshift information for two of them has been published elsewhere: N2850.4 (Smail et al. 2003) and N2850.1 (Chapman et al. 2002a).

From deep near-IR spectroscopy with the Subaru telescope, Simpson et al. (2004) have measured spectroscopic redshifts based on two or more emission lines with secure radio and near-IR identifications for two additional 8-mJy SCUBA sources (N2850.2 and N2850.12 in the ELAIS N2 Field; Scott et al. 2002). We therefore include these two sources in the expanded sample analysed here. We note that Simpson et al. also suggested a tentative redshift for LE850.3 estimated from a single 2.5σ emission line, and also a redshift for CUDSS14.9 from the putative HK Ca absorption lines that need confirmation (Simpson, private communication). These latter two redshifts are not considered robust enough for inclusion in our analysis.

2.2 New photometric redshifts

We thus have seven new redshifts for robust submm sources from the UK 8-mJy SCUBA survey, which can be added to the heterogeneous collection of eight submm sources with spectroscopic redshifts previously considered in Paper II. Thus, the new spectroscopic data have effectively doubled the size of the comparison sample, as well as extending the redshift baseline out to $z \simeq 4$.

Since our original analysis in Paper II, new photometric data at 1.2 mm obtained with MAMBO (Greve et al. 2004) have also become available for the submm galaxies first identified in the UK 8-mJy SCUBA survey areas (Scott et al. 2002). We have therefore incorporated this additional photometric information in a re-derivation of the photometric redshifts of UK 8-mJy SCUBA sources in the current spectroscopic sample. We also include N2850.12, which has a 3.4σ flux determination at 850 μm, and hence failed our selection criteria in Paper II, but which now has a spectroscopic redshift (Simpson et al. 2004) based on an IR counterpart associated with the 3σ peak in the radio observations of Ivison et al. (2002).

We have adopted the fiducial evolutionary model le2 (the least restrictive one in Paper II, which applied a non-informative prior at $z > 2.3$, and $(1+z)^3$ luminosity evolution to $z \leqslant 2.3$) to derive the new photometric redshift estimates which are given in Table 1. We produce simulated catalogues of sources in mock surveys to the same depth as those in which the real submm galaxies were detected. The corresponding redshift distributions are then derived by the joint probability of identifying the particular radio–mm–FIR colours and fluxes of the real sources with the mock galaxies in the simulated catalogues. In order to check the stability of the redshift solutions found, we have calculated 100 different Monte Carlo simulations for each source, and for each of these realizations we have derived its redshift probability distribution, its mode and 68 and 90 per cent confidence level intervals. As expected, the sources with photometric redshifts based on two or more colours are the most stable and show well-defined peaks and little variation in the mode of the redshift distribution of the different simulations. It is important to note that these photometric redshift estimates include absolute calibration errors of 5-20 per cent in the individual radio–submm

Table 1. Photometric redshifts for the sources with reported spectroscopic redshifts. The first column gives the name; the second column gives the most probable mode and the 68 per cent confidence interval for the mode among 100 Monte Carlo realizations; the third column gives the 68 per cent confidence interval for the redshift distribution of the source; the fourth one, the 90 per cent confidence interval; the fifth and sixth columns give respectively the detected bands (at a $\geqslant 3\sigma$ level) and the upper limits used for the computation of the photometric redshifts; and the seventh column gives the spectroscopic redshifts and their references: Ba99 for Barger et al. (1999); Ch02a for Chapman et al. (2002a); Ch02b for Chapman et al. (2002b); Ch02c for Chapman et al. (2002c); Ch03 for Chapman et al. (2003a); Ea00 for Eales et al. (2000); Fr98 for Frayer et al. (1998); HR94 for Hu & Ridgway (1994); Si04 for Simpson et al. (2004); and Sm03 for Smail et al. (2003).

Object	$z_{\rm phot}$ mode	68 per cent CL	90 per cent CL	$\geqslant 3\sigma$ detections	$<3\sigma$/upper limits	$z_{\rm spec}$
LH850.6	$2.6\pm^{0.4}_{0.0}$	(2.5–3.7)	(2.0–4.2)	850 μm, 1.2 mm, 1.4 GHz	450 μm, 5 GHz	2.610 (Ch03)
LH850.18	$3.8\pm^{0.2}_{0.3}$	(3.0–5.4)	(2.6–6.0)	850 μm, 1.2 mm, 1.4 GHz	450 μm,5 GHz	3.699 (Ch03)
N2850.1	$2.85\pm^{0.05}_{0.15}$	(2.5–3.8)	(2.0–4.1)	450, 850 μm, 1.4 GHz	1.2 mm	0.840 (Ch02a)
N2850.2	$2.35\pm^{0.05}_{0.15}$	(2.0–2.7)	(1.5–3.1)	450, 850 μm,1.2 mm,1.4 GHz	–	2.45 (Si04)
N2850.4	$2.6\pm^{0.1}_{0.2}$	(2.0–3.8)	(2.0–4.6)	850 μm, 1.2 mm, 1.4 GHz	450 μm	2.376 (Sm03)
N2850.8	2.5 ± 0.3	(1.5–3.5)	(1.0–4.5)	850 μm	450 μm, 1.2 mm, 1.4 GHz	1.189 (Ch03)
N2850.12	$2.5\pm^{0.2}_{0.1}$	(1.6–4.0)	(1.5–5.0)	850 μm	450 μm, 1.2 mm, 1.4 GHz	2.43 (Si04)
CUDSS14.18	$0.7\pm^{1.1}_{0.5}$	(0.3–1.5)	(0.0–1.8)	5, 1.4 GHz	450, 850 μm	0.66 (Ea00)
SMMJ02399−0134	$2.3\pm^{0.3}_{1.8}$	(1.5–3.1)	(1.0–3.8)	850 μm, 1.4 GHz	–	1.056 (Ba99)
SMMJ02399−0136	2.85 ± 0.05	(2.5–3.7)	(2.0–5.0)	450, 850 μm, 1.3 mm, 1.4 GHz	2 mm	2.808 (Fr98)
SMMJ14011+0252	$2.85\pm^{0.05}_{0.35}$	(2.0–3.3)	(2.0–4.4)	450, 850 μm, 1.3 mm, 1.4 GHz	3 mm, 2.8 GHz	2.550 (Ba99)
W−MM11	3.7 ± 1.0	(2.5–5.3)	(2.0–5.8)	850 μm	450 μm	2.98 (Ch02b)
HR10	$1.95\pm^{0.05}_{0.25}$	(1.5–2.3)	(1.5–2.9)	450, 850 μm, 1.3 mm, 8 GHz	100 μm, 1.4 GHz	1.44 (HR94)
N1−40	$0.8\pm^{0.2}_{0.3}$	(0.5–1.2)	(0.5–1.5)	175, 850 μm, 1.4 GHz	450 μm	0.45 (Ch02c)
N1−64	$1.05\pm^{0.35}_{0.25}$	(0.9–2.0)	(0.5–2.1)	175, 850 μm, 1.4 GHz	450 μm	0.91 (Ch02c)

fluxes, and assume no correlation between the luminosity and shape of an SED (or temperature).

From our sample of 15 submm galaxies, Fig. 1 shows the photometric redshift–spectroscopic redshift regression plot for those 12 sources that have at least one robust colour based on two or more detections ($\geqslant 3\sigma$) in the radio–mm–FIR regime. The remaining three sources (N2850.8, N2850.12 and W-MM11) have a robust detection at only one wavelength and various upper limits, and hence are not included in Fig. 1.

Figs 2 and 3 show the comparison of the observed SEDs of the sources analysed in this paper and the template SEDs considered in the photometric redshift analysis, illustrating the cases where there is good agreement and catastrophic disagreement, respectively. All SEDs in our template library are accepted by more than one of these sources.

2.2.1 *The case of N2850.1*

Among the photometric redshifts based on at least two colours (with well-measured fluxes, i.e. $\geqslant 3\sigma$, in three or more bands) the submm galaxy which departs most clearly from the $z_{\rm phot} = z_{\rm spec}$ line is N2850.1 ($z_{\rm phot} - z_{\rm spec} = 2.01$). Our new photometric redshift of N2850.1, using the most recent upper limit at 1.2 mm (Greve et al. 2004) together with the 450-, 850-μm and 1.4-GHz fluxes, is $z_{\rm phot} = 2.8\pm^{1.0}_{0.3}$ at a 68 per cent confidence level, and $z_{\rm phot} = 2.8\pm^{1.0}_{0.8}$ at a 90 per cent level. These values are consistent with the estimates presented in Paper II, but remain strongly inconsistent with the optical spectroscopic redshift ($z_{\rm spec} = 0.840$) reported by Chapman et al. (2003a). This is not surprising, as there has already been considerable debate over whether the optical identification for this submm source is correct. The optical spectrum and redshift for this counterpart, originally published by Chapman et al. (2002a), led these authors to argue that the optically bright galaxy coincident (within ∼0.2 arcsec) with the radio position of N2850.1 is possibly a foreground galaxy that lenses the submm source. This argument was based primarily on the fact that the temperature of the dust emission $T_{\rm D} = 23 \pm 5$ K deduced for the submm source at the optical spectroscopic redshift was 4σ below that of the local dusty galaxies with the same intrinsic luminosity. In Chapman et al. (2003a), N2850.1 has a revised temperature of $16^{+4.1}_{-2.2}$ K or 6σ below the temperature distribution of local analogues, and colder than SMM22173+0014, which Chapman et al. (2002a) also claim is lensed.

It is clear, therefore, that among the sources considered here, N2850.1 is the most likely example of a bright submm source produced by gravitational lensing by an intermediate redshift galaxy,

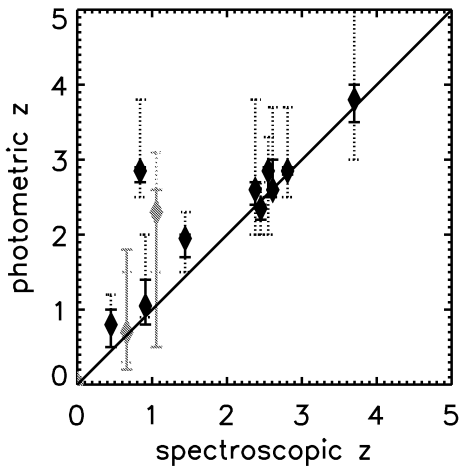

Figure 1. Comparison of the new photometric redshifts, using model le2 as a prior (see Paper II) and the true redshifts for the 12 submm sources with at least one robust radio/submm/FIR colour. The diamonds represent the most probable mode derived from 100 Monte Carlo simulations calculated for each object using model le2. The solid error bars represent the range of modes (68 per cent confidence level) measured in the corresponding redshift distributions of the 100 realizations, and the dotted lines show the 68 per cent confidence interval of a representative redshift distribution for each object. Sources represented in black (in increasing redshift: N1–40, N2850.1, N1–64, HR10, N2850.4, N2850.2, SMMJ14011+0252, LE850.6, SMMJ02399−0136 and LE850.18), have photometric redshifts derived from measurements ($\geqslant 3\sigma$) in at least three passbands of the radio–mm–FIR regime with the addition of some upper limits, and are the most precise estimates. Sources represented in dark grey (in increasing redshift: CUDSS14.18, SMMJ02399–0134) have photometric redshifts derived from measurements ($\geqslant 3\sigma$) in just two passbands and some additional upper limits.

analogous to the case of HDF850.1 studied in detail by Dunlop et al. (2004). Proving this beyond doubt remains a challenge, as astrometric information of the quality available to Dunlop et al. (2004) does not yet exist in the case of N2850.1.

Whatever the correct explanation for its properties, it is obvious that N2850.1 is an unusual source, being the only object in the sample of 15 galaxies which cannot be fitted by any of our SED templates when redshifted to $z = 0.840$ (see Fig. 3). For the sake of transparency and completeness in what follows, we therefore quote the overall accuracy of the redshift estimation procedure both with and without the inclusion of N2850.1 in the statistical calculations.

2.2.2 *Overall accuracy of photometric redshifts*

In general the agreement between photometric and spectroscopic redshifts is encouraging. The three sources for which photometric redshifts are based on a solid detection ($\geqslant 3\sigma$) at just one wavelength, however, are the least precise due to insufficient photometric constraints, although we note that they are still formally consistent with the spectroscopic redshifts found: N2850.8 at $z_{\rm spec} = 1.189$ has a photometric redshift $z_{\rm phot} = 2.5 \pm 1.0$ at a 68 per cent confidence level (1.0–4.5 at the 90 per cent level); N2850.12 has a photometric redshift of $z_{\rm phot} = 2.5^{+1.5}_{-0.9}$ at a 68 per cent confidence level (1.5 to 5.0 at the 90 per cent level), which is consistent with the $z_{\rm spec} = 2.43$ (Simpson et al. 2004); and W-MM11 at $z_{\rm spec} = 2.98$, as determined in Paper II, has a $z_{\rm phot} = 3.7^{+1.6}_{-1.2}$ at a 68 per cent confidence level (2.0–5.8 at the 90 per cent level).

Despite the strong suspicion that N2850.1 is a lensed SCUBA galaxy at a redshift $z \gg z_{\rm opt} = 0.840$, even if we include N2850.1 in our analysis the rms dispersion about $z_{\rm phot} = z_{\rm spec}$ is $\delta z = 0.38$. This result considers only those 10/15 submm galaxies with at least two measured colours based on three or more $\geqslant 3\sigma$ detections in the radio–mm–FIR regime. The precision significantly improves to $\delta z = 0.20$ if we exclude N2850.1. Extending this analysis to the 12/15 sources with at least one colour determined from detections at two or more bands, the measured mean accuracy of the photometric redshifts in the range $0.5 < z < 4$ is $\delta z = 0.42$ and $\delta z = 0.28$, including and excluding N2850.1, respectively. Finally, if we also include sources with only upper-limits in the colours (for example a single submm detection with a non-detection at radio wavelengths), we measure $\delta z = 0.48$ and $\delta z = 0.37$, including and excluding N2850.1, respectively.

3 DISCUSSION

Blain et al. (2003) have stated that the technique described in Papers I and II assumes a narrow range of local SED templates, with a tight distribution of dust temperatures, and luminosities, to derive the photometric redshifts. We emphasize again that the range of dust temperatures in our template library ranges from 25–65 K, and that we include 20 local galaxies (starbursts and AGN) with well-measured SEDs and FIR luminosities spanning the range $9.0 < \log L_{\rm FIR}\,{\rm L}_{\odot} < 12.3$. Furthermore, it is misleading to suggest that a wide range of dust temperatures (that may be correlated with luminosity) should translate directly into a similar redshift uncertainty in our calculations, as the redshift distributions are dominated by those SEDs that best fit the radio–mm–FIR data. Although all SEDs contribute to the redshift distributions at some level, but with varying degrees of significance, a well-defined peak can be measured.

The comparison presented here provides reassurance that, by allowing the variety of local template SEDs to be selected at random, and then scaled to the required FIR luminosity to populate the evolving luminosity function, we have offered the photometric redshift method a library of galaxies with a sufficiently broad range of dust temperatures, SED shapes and levels of star formation and AGN activity from which to find a solution. We also note that the sensitivities of the current submm experiments in blank field surveys select only those starburst galaxies with $L_{\rm FIR}/{\rm L}_{\odot} > 10^{11}$. This being the case, then perhaps the future choice of SEDs should be restricted to those galaxies more luminous than this sensitivity limit, in which case our library of SEDs will only be lacking the highest luminosity local counterparts ($12.3 < L_{\rm FIR}/{\rm L}_{\odot} < 13$). If we consider that there exists a luminosity–temperature dependence in the SEDs of starbursts, then we will be missing the SEDs that peak at the shortest wavelengths in our library, and thus we will be underestimating the redshifts for some fraction of SCUBA sources.

An encouraging aspect of our study is that the derived errors in our calculations of the individual photometric redshifts (i.e. the 68 per cent confidence levels, shown as dotted lines in Fig. 1 and in column 3 of Table 1), are systematically larger than the measured dispersion around the $z_{\rm phot} = z_{\rm spec}$ line. This dispersion is based on the differences between the modes of the photometric redshift distributions and the spectroscopic redshifts. For instance, the average 68 per cent confidence interval is $\delta z \approx 0.65$ for those sources with two or more colours derived from three or more detections (black diamonds in Fig. 1), while the measured accuracy of their photometric redshifts is $\delta z \approx 0.38$ and $\delta z \approx 0.20$, including and excluding N2850.1. This suggests that our errors are overestimated, possibly due to considering a range of SED templates wider than the true, but still unknown, distribution of SED shapes of submm galaxies. We note, however, that, with the currently available photometry, all the

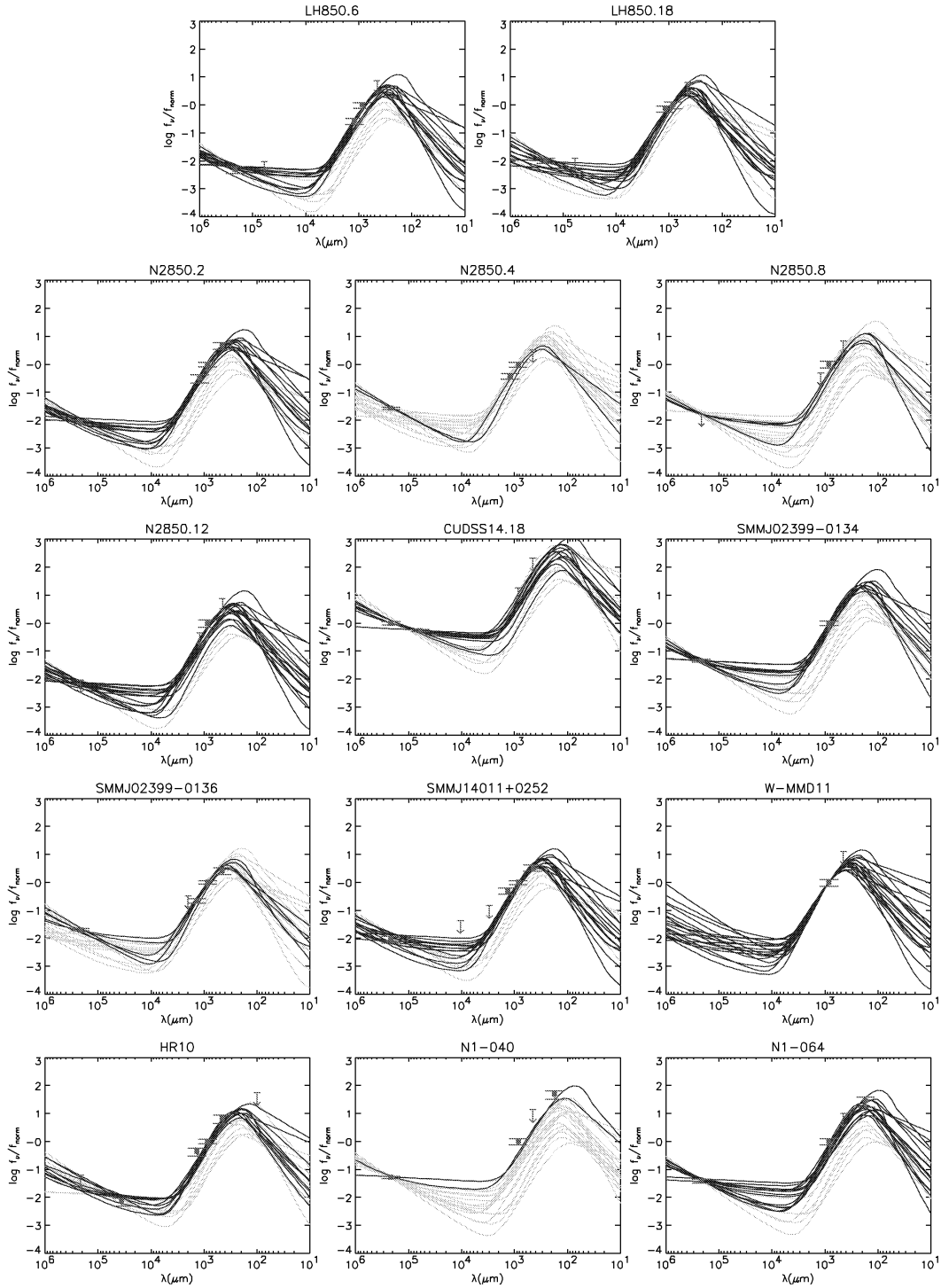

Figure 2. Observed SEDs of sources for which acceptable photometric redshifts were derived. The SEDs, normalized to the flux density at 850 μm are shown as squares and arrows. The arrows indicate 3σ upper limits. The squares denote detection at a level $\geqslant 3\sigma$, with 1σ error bars. The template SEDs (lines) are redshifted to the spectroscopic redshift published in the literature, and scaled to maximize the likelihood of detections and upper limits through survival analysis (Isobe, Feigelson & Nelson 1986). The template SEDs at this redshift compatible within 3σ with the observations of the sources are displayed as darker lines.

SEDs in our template library are accepted by more than one submm galaxy as possible counterparts (Fig. 2).

To conclude this paper, and to provide further justification for the results presented in Section 2.2, we illustrate in Fig. 4 how the accuracy of the photometric redshift method evolves and improves as we include an increasing number of robust photometric measurements. When based on a single detection at 850 μm (Fig. 4a) the initial photometric redshift estimates reflect only the prior assumption for the luminosity evolution of the submm population. The addition of detections or deep limits at $\lambda \leqslant 450$ μm, which sample the rest-frame

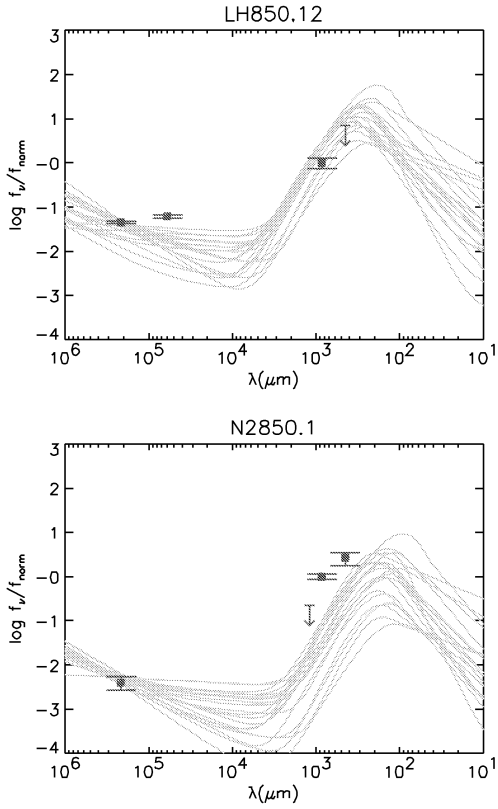

Figure 3. Observed SEDs of two submm galaxies for which catastrophic photometric redshifts were derived. Symbols and lines are as in Fig. 2. LE850.12 has been excluded from the photometric redshift analysis due to its high and variable radio flux (Section 2.1), but we show it here to demonstrate explicitly that it cannot be reproduced by any of our template SEDs. In the case of N2850.1 the SEDs are fitted under the assumption that the submm galaxy is at $z_{opt} = 0.84$ (Chapman et al. 2002a). A possible explanation (Section 2.2) for this catastrophic photometric redshift is that N2850.1 is at a higher redshift and lensed by the foreground optical galaxy at $z = 0.84$.

FIR–submm peak, place initial constraints on the photometric redshifts (Fig. 4b). The 850 μm–radio spectral index has been shown to also provide a useful one-colour measure of photometric redshifts for the submm population (e.g. Carilli & Yun 2000), with the ability to robustly identify galaxies at $z > 2$ from those at lower redshifts. Hence the use of data in the radio regime (1.4–8 GHz) in this analysis continues to improve the photometric redshift accuracy (Fig. 4c) by providing confirmation, and therefore adding more weight to the results determined from the data at $\lambda \leqslant 850$ μm. Finally, with the addition of further mm-wavelength data at 1–2 mm, we eventually derive a photometric redshift accuracy of ± 0.42 or ± 0.28 for all 12 galaxies with at least one well-measured colour if we include or reject N2850.1. respectively (Fig. 4d).

4 CONCLUSIONS

We have complemented our previous comparison of photometric redshifts and spectroscopic redshifts for eight submm galaxies (Paper II) with seven new spectroscopic redshifts (Chapman et al. 2003a; Simpson et al. 2004) and recently published MAMBO 1.2-mm data (Greve et al. 2004). The increased number of available spectroscopic redshifts for submm galaxies with sufficient accompanying rest-frame radio to FIR photometry confirms the reliability of our previous simulations and predictions for the redshifts of

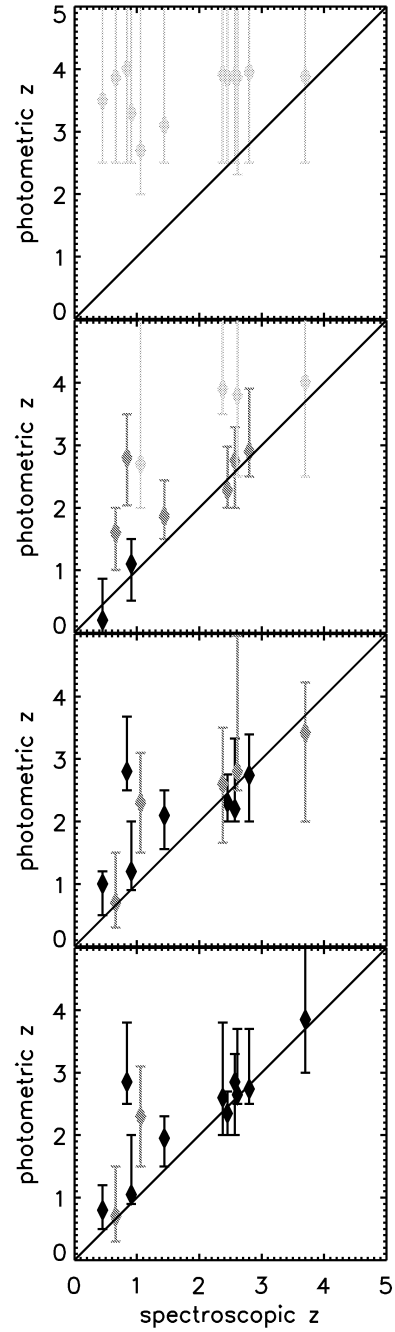

Figure 4. Dissection of the role played by progressive addition of the available photometric data in the final construction of the comparison of estimated and spectroscopic redshifts presented in Figure 1. From top to bottom, the photometric redshifts have been calculated using (a) only the 850 μm flux, (b) the 850 and 450 μm fluxes and upper limits, and if available (for N-40, N64 and HR10) also the ISO 170 μm and IRAS 100 μm fluxes and upper limits; (c) 850, 450, 170, 100 μm fluxes combined with radio data (1.4 and 8 GHz fluxes and upper limits); (d) all available data, including 1–3 mm fluxes and upper limits. The colour code indicates sources with just one robust flux determination ($\geqslant 3\sigma$) in light grey, sources with at least two robustly determined fluxes in dark grey, and sources with three or more robustly determined fluxes in black.

submm sources. This accuracy is all the more impressive given that the photometric redshifts for six of the new sources were effectively predicted before the additional seven spectroscopic redshifts were available (Paper II).

If we consider all available data for those submm galaxies that have at least one colour determination based on two detections, we conclude that the rest-frame radio–FIR photometric method can provide redshifts with an accuracy of $\sim\pm0.28$ over the redshift interval $0.5 < z < 4$. This redshift uncertainty increases to ±0.42 if the true spectroscopic redshift of the brightest submm source N2850.1 in the northern ELAIS 2 field is $z_{\rm opt} = 0.840$ (Chapman et al. 2003a). There is, however, a more natural explanation for the discrepancy between the photometric redshift and spectroscopic redshift of N2850.1, namely that the submm source is lensed by the foreground optical counterpart (as already suggested by Chapman et al. 2002a), analogous to the situation for HDF850.1, the brightest object in the *Hubble Deep Field* (Dunlop et al. 2004).

The photometric method currently relies on limited data, restricted to a few low S/N detections at observed radio, mm and submm wavelengths. No optimization of the current method has been made, based on any prior knowledge of those local SED templates that are consistent with the rest-frame data. Despite the lack of any assumption in our simulations and analysis about a dependence between the shape of a local SED and luminosity of the redshifted submm source, the method clearly works to a useful accuracy (e.g. van Kampen et al. 2005). The inclusion of such a dependence and measurements with greater S/N can only reduce the dispersion of possible SEDs that are consistent with the observational data, and hence this will reduce the width of the redshift probability distributions for individual targets.

One of the difficulties in this analysis has been to select from the limited publicly available information which submm galaxies have secure spectroscopic redshifts derived from unambiguous optical or IR counterparts. It is therefore encouraging to look forward to the next few years as the essential radio, (sub)mm and FIR photometric data become available from facilities such as the VLA, Green Bank Telescope (GBT), LMT, APEX, BLAST, Herschel, *Spitzer* and *Astro-F* for complete and substantial samples of submm sources. Thus we are confident that the combination of these high S/N multiwavelength rest-frame radio–FIR data will generate photometric redshifts with accuracies of $\Delta z \lesssim 0.3$ for the majority of the individual submm selected galaxies. Given this, it will be possible to accurately measure the entire redshift distribution and star formation history of the high-z population of heavily obscured starburst galaxies without having to measure a spectroscopic redshift for every submm source.

ACKNOWLEDGMENTS

IA and DHH gratefully acknowledge support from CONACYT grants 39548-F and 39953-F.

REFERENCES

Aretxaga I., Hughes D. H., Chapin E. L., Gaztañaga E., Dunlop J. S., Ivison R. J., 2003, MNRAS, 342, 759 (Paper II)
Barger A. J., Cowie L. L., Smail I., Ivison R. J., Blain A. W., Kneib J.-P., 1999, AJ, 117, 2656
Blain A. W., Barnard V. E., Chapman S. C., 2003, MNRAS, 338, 733
Carilli C. L., Yun M. S., 1999, Ap.J., 513, L13
Carilli C. L., Yun M. S., 2000, ApJ, 530, 618
Chapman S. C., Smail I. R., Ivison R. J., Blain A. W., 2002a, MNRAS, 335, L17
Chapman S. C., Shapley A., Steidel C., Windhorst R., 2002b, ApJ, 572, L1
Chapman S. C., Smail I., Ivison R. J., Helou G., Dale D. A., Lagache G., 2002c, ApJ, 573, 66
Chapman S. C., Blain A. W., Ivison R. J., Smail I. R., 2003a, Nat, 422, 695
Chapman S. C. et al., 2003b, ApJ, 585, 57
Devlin M., 2001, in Lowenthal J., Hughes D. H., eds, Deep Millimetre Surveys: Implications for Galaxy Formation and Evolution. World Scientific, p. 59
Dunlop J. S. et al., 2004, MNRAS, 350, 769
Dunne L., Clements D. L., Eales S. A., 2000, MNRAS, 319, 813
Eales S., Lilly S., Webb T., Dunne L., Gear W., Clements D., Yun M., 2000, AJ, 120, 2244
Frayer D. T., Ivison R. J., Scoville N. Z., Yun M., Evans A. S., Smail I., Blain A. W., Kneib J.-P., 1998, ApJ, 506, 7
Greve T. R., Ivison R. J., Bertoldi F., Stevens J. A., Dunlop J. S., Lutz D., Carilli C. L., 2004, MNRAS, 354, 779
Helou G., Soifer B. T., Rowan-Robinson M., 1985, ApJ, 289, L7
Hu E. M., Ridgway S. E., 1994, AJ, 107, 1303
Hughes D. H. et al., 1998, Nat, 394, 241
Hughes D. H. et al., 2002, MNRAS, 335, 871 (Paper I)
Isobe T., Feigelson E. D., Nelson P. I., 1986, ApJ, 306, 490
Ivison R. J. et al., 2002, MNRAS, 337, 1
Mortier A. et al., 2005, MNRAS, submitted
Rengarajan T. N., Takeuchi T. T., 2001, PASJ, 53, 433
Richards E. A., 2000, ApJ, 533, 611
Scott S. et al., 2002, MNRAS, 331, 817
Simpson C., Dunlop J. S., Eales S. A., Ivison R. J., Scott S. E., Lilly S. J., Webb T. M. A., 2004, MNRAS, 353, 179
Smail I., Chapman S. C., Ivison R. J., Blain A. W., Takata T., Heckman T. M., Dunlop J. S., Sekiguchi K., 2003, MNRAS, 342, 1185
van Kampen E. et al. 2005, MNRAS, in press (doi:10.1111/j.1365-2966.2005.08899) (astro-ph/0408552)
Wiklind T., 2003, ApJ, 588, 736
Yun M. S., Carilli C. L., 2002, ApJ, 568, 88

This paper has been typeset from a TEX/LATEX file prepared by the author.